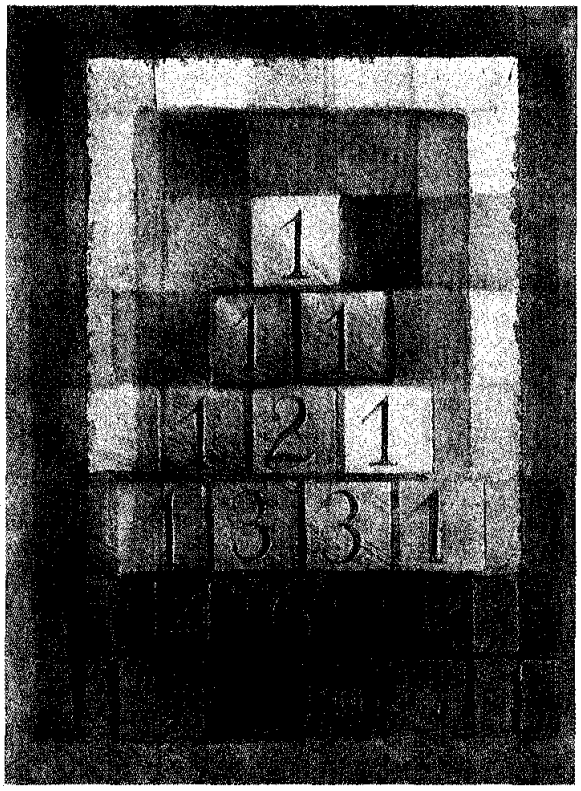

©Annette Unser

Splines

A Perfect Fit for Signal and Image Processing

Michael Unser

Finding a general mechanism for switching between the continuous and discrete signal domains is one of the fundamental issues in signal processing. It is a question that arises naturally during the acquisition process where an analog signal or image is to be converted into a sequence of numbers (discrete representation). Conversely, the need for a continuous signal representation comes up every time one wishes to implement numerically an operator that is initially defined in the continuous domain. Typical examples in image processing are the detection of edges through the computation of gradients (spatial derivatives), and geometric transformations such as rotations and scaling (interpolation).

The textbook approach to those problems is provided by Shannon's sampling theory, which describes an equivalence between a band-limited function and its equidistant samples taken at a frequency that is superior or equal to the Nyquist rate [76]. Even though this theory has had an enormous impact on the field, it still has a number of problems. First, it relies on the use of ideal filters, which are devices not commonly found in nature. Second, the band-limited hypothesis is in contradiction with the idea of a finite (or finite duration) signal. Third, the bandlimiting operation tends to generate Gibbs oscillations, which can be visually disturbing in images. Finally, the underlying cardinal basis function [$\mathrm{sinc}(x)$] has a very slow decay, which makes computations in the signal do-

1053-5888/99/$10.00©1999IEEE

main very inefficient. While the first two problems can be dealt with by using approximations and introducing concepts such as an *essential bandwidth* and an *essential time duration* [78], there is no way to address the last two issues other than changing basis functions.

Our purpose here will be to provide arguments in favor of an alternative approach that uses splines, which is equally justifiable on a theoretical basis, and which offers many practical advantages. To reassure the reader who may be afraid to enter new territory, we must emphasize that we are not losing anything because we will retain the traditional theory as a particular case (i.e., a spline of infinite degree). The basic computational tools will also be familiar to a signal processing audience (filters and recursive algorithms), even though their use in the present context is less conventional. In the course of the presentation, we will also bring out the connection with the multiresolution theory of the wavelet transform.

Interestingly, splines are slightly older than Shannon's sampling theory. They were first described in 1946 [70]. In his landmark paper, Schoenberg laid the mathematical foundations for the subject; he showed how one could use splines to interpolate equally spaced samples of a function. He also introduced the B-splines, the basic atoms by which polynomial splines are constructed. Despite this early start, the subject of splines then lay more or less dormant during the 1950s, while signal processing developed at a rapid pace within Shannon's elegant framework of band-limited functions. Splines only really took off in the early 1960s when mathematicians realized that these functions could model the physical process of drawing a smooth curve (minimum curvature property). This created an intense interest in the subject and the applications soon followed in approximation theory [24], [74], numerical analysis [64], and various other branches of applied mathematics [3]. With the advent of digital computers, splines caught the interest of engineers and had a tremendous impact on computer-aided design [29], [45] and computer graphics [10]. However, there was little crossover to signal processing, perhaps because researchers in this field had become so accustomed to thinking in terms of band-limited functions. Recently, thanks in part to a new (non-band-limited) way of thinking brought forth by wavelet theory [51], the situation has changed significantly.

This article attempts to fullfill three goals. The first is to provide a tutorial on splines that is geared to a signal processing audience. The second is to gather all their important properties and provide an overview of the mathematical and computational tools available; i.e., a road map for the practitioner with references to the appropriate literature. The third goal is to give a review of the primary applications of splines in signal and image processing; most of those are discussed in the final part of the article.

Spline Interpolation

Polynomial Splines

Splines are piecewise polynomials with pieces that are smoothly connected together. The joining points of the polynomials are called *knots*. For a spline of degree n, each segment is a polynomial of degree n, which would suggest that we need $n+1$ coefficients to describe each piece. However, there is an additional smoothness constraint that imposes the continuity of the spline and its derivatives up to order $(n\text{-}1)$ at the knots, so that, effectively, there is only one degree of freedom per segment. Here, we will only consider splines with uniform knots and unit spacing. The remarkable result, due to Schoenberg [70], is that these splines are uniquely characterized in terms of a B-spline expansion

$$s(x)=\sum_{k\in Z} c(k)\beta^n(x-k), \tag{1}$$

which involves the integer shifts of the central B-spline of degree n denoted by $\beta^n(x)$; the parameters of the model are the B-spline coefficients $c(k)$. B-splines, defined below, are symmetrical, bell-shaped functions constructed from the $(n+1)$-fold convolution of a rectangular pulse β^0:

$$\beta^0(x)=\begin{cases}1, & -\frac{1}{2}<x<\frac{1}{2}\\ \frac{1}{2}, & |x|=\frac{1}{2}\\ 0, & \text{otherwise}\end{cases} \tag{2}$$

$$\beta^n(x)=\underbrace{\beta^0*\beta^0*\cdots*\beta^0}_{(n+1)\text{ times}}(x). \tag{3}$$

The B-splines of degrees 0 to 3 are shown in Fig. 1. Since the B-spline model (1) is linear, studying the properties of the basic atoms can tell us a lot about splines in general (cf. Box 1). Thanks to this representation, each spline is unambiguously characterized by its sequence of B-spline coefficients $c(k)$, which has the convenient structure of a discrete signal, even though the underlying model is continuous (discrete/continuous representation).

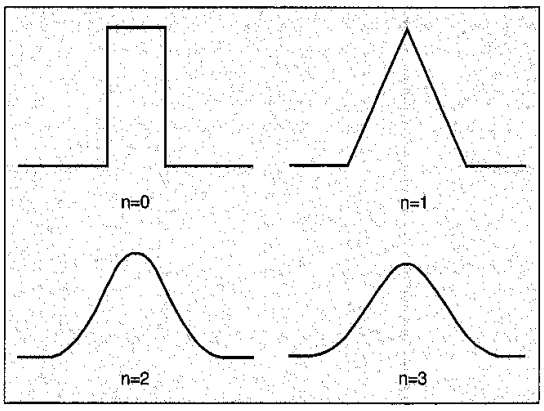

▲ *1. The centered B-splines of degree 0 to 3.*

B-splines are very easy to manipulate. For instance, we can obtain derivatives through the following formula

$$\frac{d\beta^n(x)}{dx} = \beta^{n-1}\left(x+\tfrac{1}{2}\right) - \beta^{n-1}\left(x-\tfrac{1}{2}\right), \tag{4}$$

which reduces the degree by one. Similarly, we compute the integral as

$$\int_{-\infty}^{x} \beta^n(x)dx = \sum_{k=0}^{+\infty} \beta^{n+1}\left(x-\tfrac{1}{2}-k\right). \tag{5}$$

Once we know the effect of linear operators such as (4) or (5) on the basis functions, it is a trivial matter to apply them to any spline via the B-spline representation (1).

Within the family of polynomial splines, cubic splines tend to be the most popular in applications—perhaps due to their minimum curvature property, which is discussed in "Variational Properties." Using (2), we obtain the following closed-form representation of the cubic B-spline

$$\beta^3(x) = \begin{cases} \frac{2}{3} - |x|^2 + \frac{|x|^3}{2}, & 0 \le |x| < 1 \\ \frac{(2-|x|)^3}{6}, & 1 \le |x| < 2 \\ 0, & 2 \le |x|, \end{cases} \tag{6}$$

which is often used for performing high-quality interpolation.

B-Spline Interpolation via Digital Filtering

From what has been said so far, it appears that most of the work consists in determining the B-spline model of a given input signal $s(k)$. We now consider the spline *interpolation* problem where the coefficients are determined such that the function goes through the data points exactly (cf. Fig. 2). For splines of degree 0 (piecewise constant) and splines of degree 1 (piecewise linear), this is a trivial matter because the B-spline coefficients are identical to the signal samples: $c(k)=s(k)$. For higher-degree splines, however, the situation is more complex. Traditionally, the B-spline interpolation problem has been approached using a matrix framework—setting up a band-diagonal system of equations, which is then solved using standard numerical techniques (forward/backward substitution or LU decomposition) [25], [64]. In the early 1990s, it was recognized that this problem (as well as many other related ones) could also be approached using simpler digital filtering techniques [33], [93], [96], [97].

To derive this type of signal processing algorithm, we need to introduce the discrete B-spline kernel b_m^n, which is obtained by sampling the B-spline of degree n expanded by a factor of m:

$$b_m^n(k) = \beta^n(x/m)\Big|_{x=k} \quad \overset{z}{\leftrightarrow} \quad B_m^n(z) = \sum_{k\in Z} b_m^n(k) z^{-k}. \tag{11}$$

Box 1. B-Splines

The B-splines (where the B may stand for *basis* or *basic*) are the basic building blocks for splines. Their usefulness stems from the fact that they are compactly supported; in fact, they are the shortest possible polynomial splines [72]. Here, we consider the center-symmetric B-spline of degree n, $\beta^n(x)$, defined by (2) and (3). The simplest way to obtain an explicit formula is to start by writing its Fourier transform

$$\hat{\beta}^n(\omega) = \left(\frac{\sin(\omega/2)}{(\omega/2)}\right)^{n+1} = \frac{(e^{j\omega/2} - e^{-j\omega/2})^{n+1}}{(j\omega)^{n+1}}, \tag{7}$$

where we have expressed the $(n+1)$-fold convolution in (3) as a product in the frequency domain. Let us now consider the one-sided power function

$$(x)_+^n = \begin{cases} x^n, & x \ge 0 \\ 0, & x < 0 \end{cases}, \tag{8}$$

whose Fourier transform we denote by $X_+^n(\omega)$. In order to avoid evaluating $X_+^n(\omega)$ explicitly (because this involves Dirac deltas), we differentiate $(x)_+^n$ repeatedly until we hit the $(n+1)$th order discontinuity at the origin: $D^{n+1}(x)_+^n = n!\delta(x)$. In the Fourier domain, this gives $(j\omega)^{n+1} X_+^n(\omega) = n!$. Using this identity, we manipulate (7) as follows

$$\hat{\beta}^n(\omega) = \frac{(e^{j\omega/2} - e^{-j\omega/2})^{n+1}}{(j\omega)^{n+1}} \underbrace{\frac{(j\omega)^{n+1} X_+^n(\omega)}{n!}}_{=1}$$

$$= \frac{1}{n!}(e^{j\omega/2} - e^{-j\omega/2})^{n+1} X_+^n(\omega).$$

Next, we expand the term in parentheses using the binomial theorem, which yields

$$\hat{\beta}^n(\omega) = \frac{1}{n!}\sum_{k=0}^{n+1}\binom{n+1}{k}(-1)^k e^{-j\omega[k-(n+1)/2]} X_+^n(\omega). \tag{9}$$

Finally, we interpret the complex exponentials as pure phase factors (time shifts), and obtain the corresponding time domain formula

$$\beta^n(x) = \frac{1}{n!}\sum_{k=0}^{n+1}\binom{n+1}{k}(-1)^k\left(x-k+\frac{n+1}{2}\right)_+^n. \tag{10}$$

This result clearly shows that $\beta^n(x)$ is a piecewise polynomial of degree n. It also implies that the $(n+1)$th derivative of $\beta^n(x)$ is a series of Dirac impulses, indicating that $\beta^n(x)$ is differentiable up to order n. For n odd, the knots (or points of discontinuity of the nth derivative) are on the integers, while for n even, they are at the half integers.

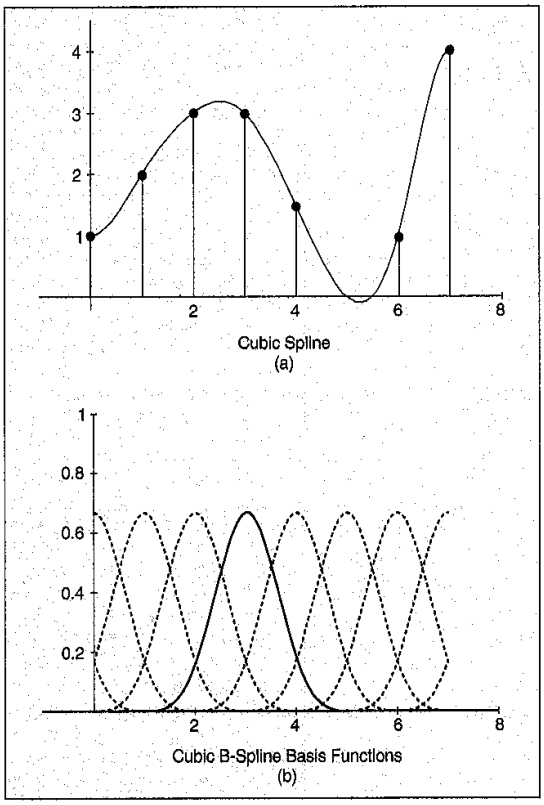

▲ *2. Example of a cubic spline signal that is represented as a linear combination of shifted cubic B-splines. Given the signal's samples, the basic problem is to determine the appropriate coefficients in (1).*

Now, given the signal samples $s(k)$, we want to determine the coefficients $c(k)$ of the B-spline model (1) such that we have a perfect fit at the integers; i.e., $\forall k \in Z$,

$$\sum_{l\in Z} c(l)\beta^n(x-l)\big|_{x=k} = s(k).$$

Using the discrete B-splines, this constraint can be rewritten in the form of a convolution

$$s(k) = (b_1^n * c)(k). \tag{12}$$

Defining the inverse convolution operator

$$(b_1^n)^{-1}(k) \overset{z}{\leftrightarrow} 1/B_1^n(z),$$

the solution is found by inverse filtering (cf. [97])

$$c(k) = (b_1^n)^{-1} * s(k). \tag{13}$$

Since b_1^n is symmetric FIR (finite impulse response), the so-called direct B-spline filter $(b_1^n)^{-1}$ is an all-pole system that can be implemented very efficiently using a cascade of first-order causal and anti-causal recursive filters [93], [96]. This algorithm is stable numerically and is faster and easier to implement than any other numerical technique. The explicit procedure for the cubic spline case is described in Box 2.

Cardinal Splines

To bring out the connection between the spline interpolation process and the traditional approach for band-limited functions, it is helpful to introduce the cardinal spline basis functions that are the spline analogs of the sinc function. Combining (1) and (13), we have

$$\begin{aligned} s(x) &= \sum_{k\in Z}\left((b_1^n)^{-1} * s\right)(k)\beta^n(x-k) \\ &= \sum_{k\in Z} s(k) \sum_{l\in Z} (b_1^n)^{-1}(l)\beta^n(x-l-k) \\ &= \sum_{k\in Z} s(k)\eta^n(x-k), \end{aligned} \tag{14}$$

where we have identified the cardinal spline of degree n:

$$\eta^n(x) = \sum_{k\in Z} (b_1^n)^{-1}(k)\beta^n(x-k). \tag{15}$$

Thus, (14) provides a spline interpolation formula that uses the signal values as coefficients. The formula works because $\eta^n(x)$ has the same interpolation property as the sinc function; it vanishes for all integers except at the origin, where it takes the value one. The cardinal spline represents the impulse response of the corresponding spline interpolator. Note that, for $n \geq 2$, these functions are no longer compactly supported; however, they decay exponentially fast. We can also express (15) in the Fourier domain, which yields the frequency response of the spline interpolator of degree n

$$H^n(\omega) = \left(\frac{\sin(\omega/2)}{\omega/2}\right)^{n+1} \frac{1}{B_1^n(e^{j\omega})}. \tag{16}$$

The cardinal cubic spline is shown in Fig. 4 and appears to be quite similar to the sinc function. In fact, it has been shown that $\eta^n(x)$ converges to sinc(x) as n goes to infinity [7]. It is a rather strong type of convergence (L_p-norm) that holds in both time and frequency domains (cf. Fig. 5).

Note that the correspondence between splines of infinite order and band-limited functions was known to Schoenberg and his successors [27], [73]. However, these mathematical results did not reach the signal processing community until recently [7], mainly due to substantial differences in context and terminology. Approximation theorists typically speak of "entire functions of exponential type" when they refer to band-limited functions. The recent cross-fertilization that has occurred has been quite fruitful and there have been benefits on both sides. For instance, the idea of using an anti-aliasing filter in Shannon's sampling theory has suggested similar solutions for splines; these are discussed in the next section.

We should emphasize that the primary usefulness of the cardinal splines is conceptual. They provide us with a better understanding of the algorithm. From a practical

Box 2. Fast Cubic Spline Interpolation

By sampling the cubic B-spline (6) at the integers, we find that

$$B_1^3(z) = (z + 4 + z^{-1})/6.$$

Thus, the filter to implement is

$$(b_1^3)^{-1}(k) \overset{z}{\leftrightarrow} \frac{6}{z+4+z^{-1}} = 6\left(\frac{1}{1-z_1 z^{-1}}\right)\left(\frac{-z_1}{1-z_1 z}\right),$$

with $z_1 = -2+\sqrt{3}$. Given the input signal values $\{s(k)\}_{k=0,\ldots,N-1}$ and defining $c^-(k) = c(k)/6$, the right-hand-side factorization leads to the following recursive algorithm

$$c^+(k) = s(k) + z_1 c^+(k-1), \quad (k = 1,\ldots,N-1)$$

$$c^-(k) = z_1\left(c^-(k+1) - c^+(k)\right), \quad (k = N-2,\ldots,0),$$

where the first filter is causal, running from left to right, while the second is anti-causal running from right to left (cf. Fig. 3). We also have to specify the appropriate starting values for the two recursions; i.e., $c^+(0)$ and $c^-(N-1)$. To ensure that the procedure is reversible, we use mirror-symmetric boundary conditions; i.e., $s(k) = s(l)$ for $(k+l) \bmod (2N-2) = 0$. The requirement is that $s(k)$ can be recovered exactly by convolving $c(k)$ with b_1^3 using the same type of boundary conditions. The resulting "folded" signal is defined for $k \in Z$ and is periodic with period $2N-2$. Using the fact that the impulse response of the first causal filter is an exponential, we may pre-calculate the initial value for the first recursion exactly:

$$c^+(0) = \sum_{k=0}^{+\infty} s(k) z_1^k = \sum_{i=0}^{+\infty} \left(z_1^{2N-2}\right)^i \sum_{k=0}^{2N-3} s(k) z_1^k$$

$$= \frac{1}{1-z_1^{2N-2}} \sum_{k=0}^{2N-3} s(k) z_1^k.$$

In practice, we use $c^+(0) = \sum_{k=0}^{k_0} s(k) z_1^k$, with $k_0 > \log\varepsilon / \log|z_1|$ where ε is the desired level of precision. For the second recursion, we apply a more efficient (in-place) initialization

$$c^-(N-1) = \frac{z_1}{(1-z_1^2)}\left(c^+(N-1) + z_1 c^+(N-2)\right),$$

which is exact for the underlying signal extension; it takes advantage of previously calculated values and is based on an alternative decomposition of the transfer function in sums of partial fractions [96].

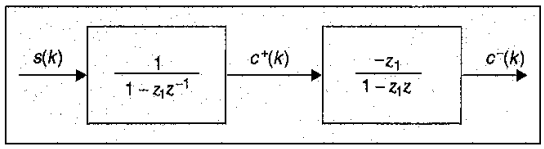

▲ *3. Recursive causal and anti-causal filters for cubic spline interpolation.*

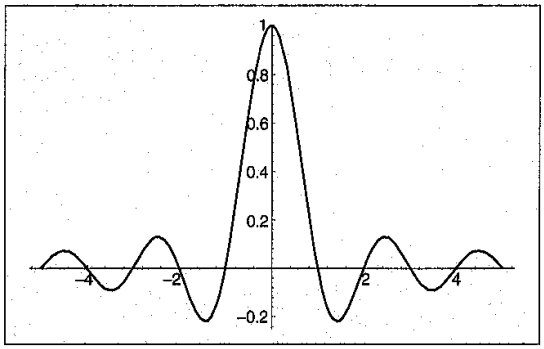

▲ *4. Cardinal (or fundamental) cubic spline.*

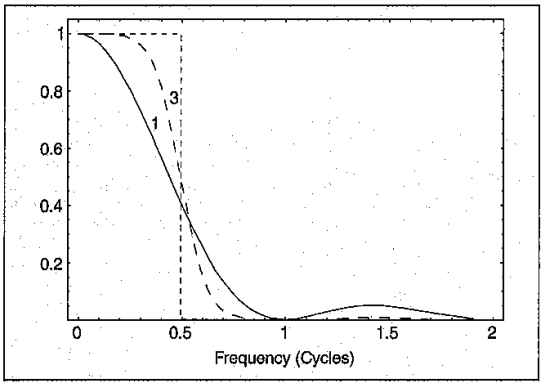

▲ *5. Frequency response of the spline interpolators of degree n=1 and 3. As n increases, the spline interpolators tend to the ideal low-pass filter (dotted line).*

point of view, however, it is much more efficient to work with the B-spline representation, at least when we are performing interpolation. The reason for this is that, in most applications, it is the re-sampling part (evaluation of the expansion formula (1) or (17)) that is by far the most costly step. Accordingly, we have the advantage of using the shortest possible basis functions (i.e., B-splines) such that the number of terms that contribute for a given x is minimized. This is precisely why splines are so much more computationally efficient than the traditional sinc-based approach. Because sinc(x) decays like $1/|x|$, computing a signal value at a particular non-integer location with an error of less than 1% will require of the order of 100 operations in each direction, while B-splines provide an exact computation with just a few non-zero terms ($n+1$ to be precise). (In q-dimensions, the complexity of an interpolation algorithm that uses separable basis functions increases with the power of q. For this reason, virtually no one uses sinc interpolation for images, not to mention volumes.) An illustration of how these ideas can apply for the geometric transformation of images is given in Box 3. When compared to any other type of

Box 3. Application-Geometric Transformation of Images

It is easy to extend splines to higher dimensions by using tensor-product basis functions. Specifically, the spline model for a particular location (x,y) in the image is given by

$$f(x,y)=\sum_{k=k_1}^{(k_1+K-1)}\sum_{l=l_1}^{(l_1+K-1)} c(k,l)\beta^n(x-k)\beta^n(y-l), \quad (17)$$

with

$$k_1=k_1(x)=\left\lceil x-\frac{n+1}{2}\right\rceil,$$

$$l_1=l_1(y)=\left\lceil y-\frac{n+1}{2}\right\rceil,$$

and

$$K=\text{support}\{\beta^n\}=n+1.$$

Here, we have restricted the summation range explicitly to those contributions that are non-zero at the particular location (x,y).

Assume now that we wish to transform the image geometrically according to a mapping $(x,y)=G(u,v)$ where (u,v) are the new image coordinates (destination). For example, the mapping may be a rotation in which case the operator G is described by a 2×2 orthogonal matrix. The B-spline transformation algorithm is as follows: First, we start by precomputing the B-spline coefficients $c(k,l)$ by separable filtering of the pixel values $f(k,l)$. In other words, we apply the 1D filtering algorithm in Box 2 successively along the rows and columns of the image. Second, we scan through the image points in the transformed representation. At each location (u,v) in the destination, we determine the corresponding location (x,y) in the source and compute the actual image value according to (17). This process typically requires the computation of $2(n+1)$ basis function values (due to separability) plus $2(n+1)^2$ multiplications per point. Note that the cost of the prefiltering step is negligible in comparison (e.g., on the order of four operations per pixel value in the cubic spline case—one operation = one multiplication + one addition; this count assumes that the B-splines are denormalized). It is possible to use as high an order as one wishes, but there is usually not much benefit beyond cubic splines.

interpolator, B-splines offer the best performance for the least complexity (we discuss this issue in more depth later in the article).

It is worth mentioning that many authors in image processing leave out the essential prefiltering step in Box 3. This has a catastrophic effect on performance and perpetuates the incorrect belief that high-order B-spline interpolation results in increased image blurring. By looking at the frequency responses in Fig. 5, the reader will be convinced that this cannot be the case. In fact, using a high-degree spline interpolator (typ., $n=5$) is a good, stable computational way of approximating the ideal sinc interpolator. For a given computational budget, it is usually superior to using a windowed sinc function, especially in high dimensions [84]. The spline approach wins because it has a high order of approximation (cf. "Controlling the Approximation Error") and an effective, sinc-like impulse response that is infinite (thanks to the IIR prefiltering step).

Spline Sampling Theory

Most of the developments in this area are relatively recent and have greatly benefited from the analogy of the traditional approach dictated by Shannon's sampling theory which recommends the use of an anti-aliasing filter when the input signal is not band-limited [38], [95]. The concepts are best explained from the general perspective of Hilbert spaces [6]. For convenience, we will use a slightly more general spline generating function, which we represent as

$$\varphi(x)=\sum_{k\in Z} p(k)\beta^n(x-k), \quad (18)$$

with the important restriction that the sequence p is such that the integer translations of φ form a basis of our basic spline space. (The necessary and sufficient condition for having a Riesz basis is that $0<|P(e^{j\omega})|<+\infty$, where $P(e^{j\omega})$ is the Fourier transform of the sequence $p(k)$ [6]). The two special cases that we have in mind are the B-splines, with $p(k)=\delta[k]$ (the Kronecker delta), and the cardinal splines with $p=(b_1^n)^{-1}$. Since we are also interested in varying the sampling step, we define the spline space of degree n with step size T by rescaling the basic model in (1)

$$S_T^n=\left\{s_T(x)=\sum_{k\in Z} c(k)\varphi(x/T-k): c(k)\in l_2\right\}. \quad (19)$$

These splines with step size T are formed by taking linear combinations of the generalized spline basis functions rescaled by a factor T and spaced accordingly. As before, there is exactly one coefficient $c(k)$ per knot or sampling point. The condition $c(k)\in l_2$ means that we are restricting ourselves to linear combinations with a finite energy. In this way, we are ensuring that S_T^n is a well-defined subspace of L_2, the space of all finite energy functions. Note that the space L_2 is considerably larger than $B_\pi=S_1^\infty$, the traditional subspace of band-limited functions considered in signal processing. To use an analogy, L_2 is to B_π (or S_1^n) as R (the real numbers) is to Z (the integers).

Spline Sampling via an Appropriate Prefilter

Now, we are interested in approximating an arbitrary signal $s(x)$ by a spline $s_T\in S_T^n$. As a measure of error, we use the L_2-norm $\|s-s_T\|_{L_2}$, which is induced by the L_2-inner product:

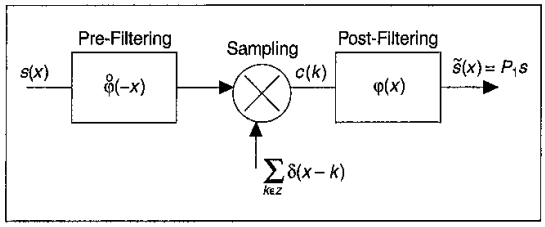

▲ *6. Least-squares spline approximation. The analog input signal s(x) is prefiltered with $\mathring{\varphi}(-x)$ and sampled thereafter to yield the generalized spline coefficients $c(k) = \langle s(x), \mathring{\varphi}(x-k) \rangle$. The sampling is modeled by a multiplication with a sequence of Dirac deltas. The spline approximation $\tilde{s}(x) = \sum_{k\in Z} c(k)\varphi(x-k)$ is then obtained by post-filtering with $\varphi(x)$.*

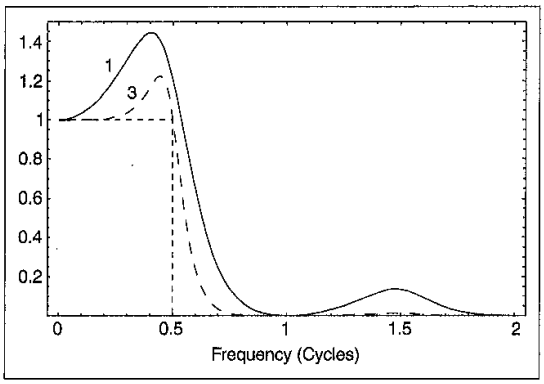

▲ *7. Frequency response of the optimal spline prefilters of degree n=1 and 3. As n increases, the optimal spline prefilters tend to the ideal low-pass filter (dotted line).*

$$\langle f, g \rangle = \int_{-\infty}^{+\infty} f^*(x) g(x) dx \quad \text{and} \quad \|f\|_{L_2} = \langle f, f \rangle^{\frac{1}{2}}, \tag{20}$$

According to this criterion, the minimum error approximation of $s(x) \in L_2$ in S_T^n is given by its orthogonal projection onto S_T^n. Using the property that the corresponding approximation error $s(x) - s_T(x)$ must be orthorgonal to S_T^n, it is not too difficult to show that the coefficient of the best approximation (least-squares solution) are given by (cf. [95])

$$c_T(k) = \frac{1}{T} \left\langle s(x), \mathring{\varphi}(x/T - k) \right\rangle. \tag{21}$$

where $\mathring{\varphi}(x) \in S_1^n$ is the dual of $\varphi(x)$, in the sense that

$$\left\langle \mathring{\varphi}(x-k), \varphi(x-l) \right\rangle = \delta[k-l]$$

(bi-orthogonality condition). While this may sound rather abstract, there is a simple prefiltering and sampling interpretation of (21). The corresponding block diagram for the simplified case of a unit sampling step $T=1$ is shown in Fig. 6.

This is similar to the conventional sampling procedure dictated by Shannon's theory except that the optimal prefilter, which is the time-reversed version of $\mathring{\varphi}(x)$, is not necessarily ideal. In the particular case of the cardinal representation where the spline coefficients are the signal samples (i.e., $p = (b_1^n)^{-1}$), the transfer function of the optimal prefilter is given by (cf. [95])

$$\mathring{H}^n(\omega) = \left(\frac{\sin(\omega/2)}{\omega/2} \right)^{n+1} \frac{B_1^n(e^{j\omega})}{B_1^{2n+1}(e^{j\omega})}, \tag{22}$$

where $B_1^p(e^{j\omega})$ is the Fourier transform of a discrete B-spline of degree p [cf. (11)].

The frequency responses of the optimal prefilter for the cardinal spline representations of increasing degrees are shown in Fig. 7. The low-pass character of the response suggests that the prefilter $\mathring{\varphi}(x)$ has a role analogous to that of the anti-aliasing filter required in conventional sampling theory. In fact, as the order of the spline goes to infinity, both $H^n(\omega)$ and $\mathring{H}^n(\omega)$ [cf. (16) and (22)] converge to the ideal low-pass filter (dotted lines in Fig. 7) [95], which is consistent with the fact that a band-limited signal can also be viewed as a spline of infinite degree (i.e., $B_\pi = S_1^\infty$).

Controlling the Approximation Error

We have just seen that there is no fundamental difference between the process of performing a least-squares spline approximation of a signal and obtaining its band-limited representation using the standard sampling procedure dictated by Shannon's theory. The only difference is in the choice of the appropriate analog prefilter. So far so good, but how should we choose the sampling step T? Is there any equivalent of the sampling theorem that tells us that the signal can be reconstructed exactly if it is sampled at a frequency $1/T$ that is at least twice the Nyquist rate $\omega_{max}/(2\pi)$? In principle, one should expect a similar result, at least for higher-order splines.

Because we are performing an orthogonal projection, the approximation error will be generally non-zero unless the signal is already included in our approximation space. However, we can hope to control this error by choosing a sampling step T that is sufficiently small. To analyze this situation, which is more complicated than in the traditional band-limited case, we turn to approximation theory. A fundamental result is that the rate of decay L of the error as a function of T depends on the ability of the representation to reproduce polynomials of degree $n=L-1$. The approximation error also depends on the bandwidth of the signal. The relevant measure in this context is

$$\left\| s^{(L)} \right\| = \left(\frac{1}{2\pi} \int_{-\infty}^{+\infty} \omega^{2L} \left| \hat{s}(\omega) \right|^2 d\omega \right)^{\frac{1}{2}}, \tag{23}$$

where $\hat{s}(\omega)$ denotes the Fourier transform of s; this is nothing but the norm of the Lth derivative of s. The key result from the Strang-Fix theory of approximation is the following error bound (cf. [40, 80]):

$$\forall s \in W_2^L, \quad \|s - P_T s\| \leq C_L \cdot T^L \cdot \left\|s^{(L)}\right\|, \tag{24}$$

where $P_T s$ is the least-squares spline approximation of s at sampling step T and C_L is a known constant. W_2^L denotes the space of functions that are L times differentiable in the L_2, or finite-energy sense. In other words, the error will decay like $O(T^L)$, where the order $L=n+1$ is one more than the degree n. Spline interpolation gives the same rate of decay as the least-squares approximation (21), but with a larger leading constant [103].

Recently, it has become possible to determine the approximation error much more precisely by simply integrating the whole spectrum of the function to approximate against a frequency kernel $E^n(\omega)$ [15]. The justification for this procedure is the error formula

$$\forall s(x) \in W_2^r,$$

$$\|s - P_T s\| = \left[\frac{1}{2\pi}\int_{-\infty}^{+\infty} E^n(T\omega)\left|\hat{s}(\omega)\right|^2 d\omega\right]^{\frac{1}{2}} + \gamma T^r \left\|s^{(r)}\right\|_{L_2}, \tag{25}$$

where $|\gamma|$ is bounded by some known constant [13]. The second term in (25) is a correction that may take positive or negative values. It is zero for band-limited functions and very small otherwise, provided that $s(x)$ is sufficiently smooth ($s(x) \in W_2^r$ with r large). Moreover, the second term cancels out if we take the average approximation error over all possible shifts of the input function; this is a reasonable thing to do since the sampling phase is usually arbitrary. Thus, the first term on the right-hand side in (25) provides a very accurate prediction of the error, which can be the basis for a quantitative Fourier domain evaluation [15]. The error kernel for a least-squares spline approximation of degree n is

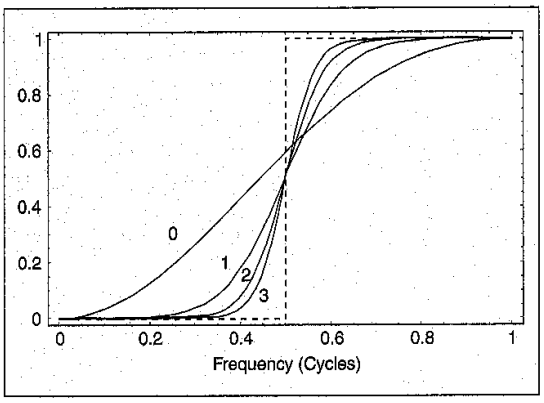

▲ *8. Frequency plot of the error kernels for the least-squares spline approximations of degree n=0,1,2,3. Below the Nyquist frequency $\omega = \pi$, the kernels (and therefore the errors) tend to be smaller for splines of higher degree.*

$$E^n(\omega) = 1 - H^n(\omega)\overset{\circ}{H}{}^n(\omega). \tag{26}$$

where $H^n(\omega)$ and $\overset{\circ}{H}{}^n(\omega)$ are the spline filters defined by (16) and (22), respectively. The main point is that the study of these kernels gives us a very direct way to assess the performance of the various types of spline approximations. This approach is simple, intuitive, and yet powerful enough to recover all classical results and L_2-bounds in approximation theory [e.g. (24)]. We have plotted the error kernels for $n=0$, to 3 in Fig. 8. This graph clearly shows that for signals that are predominantly low-pass (i.e., with a frequency content within the Nyquist band), the error tends to be smaller for higher-order splines.

The order property (24) is a direct consequence of the degree of flatness of the kernel around the origin. Specifically, for an Lth order spline, $E^n(\omega)$ has $2L-1$ vanishing derivatives at $\omega = 0$. This implies that

$$E^n(T\omega) = (C_L \cdot T^L \cdot \omega^L)^2 + O(T^{2L+2}\omega^{2L+2})$$

as $\omega \to 0$, which explains the $O(T^L)$ behavior of the error described by (24) (for more details, refer to [15]).

As the graph in Fig. 8 also suggests, the error approaches that of a band-limited approximation as the order of the spline increases, which again reinforces the analogy with Shannon's sampling theorem. In the limit as $n \to +\infty$, the product $H^n(\omega)\overset{\circ}{H}(\omega)$ tends to the ideal low-pass filter, so that we end up with an error entirely due to the out-of-band frequency content of the signal. The implication is that higher-order splines will usually produce better approximations in the L_2-norm, although this may occur at the expense of ringing artifacts as the model gets closer to being band-limited.

Multiresolution Spline Processing

Consider a spline with knots at the integers and dilate it by an integer factor m. The resulting enlarged function is clearly piecewise polynomial in each unit interval, which means that it is also a spline with respect to the initial integer grid. This simple observation is the key to the multiresolution properties of splines, which makes them perfect candidates for the construction of wavelets and pyramids. Here, we will emphasize the special two-scale relation for splines, and the construction of pyramids (we touch on the subject of wavelets only briefly here). We will also briefly make the connection between splines and wavelets.

m-Scale Relation

For the above scale-invariance argument to hold, we need the spline knots to be positioned on the integers. To simplify the discussion, we will momentarily consider the shifted causal B-splines

$$\varphi^n(x) = \beta^n\left(x - \tfrac{n+1}{2}\right), \tag{27}$$

which have the required property. Similar to the centered B-splines (3), these can also be constructed from the $(n+1)$-fold convolution of φ^0, the indicator function in the unit interval. Clearly, $\varphi^0(x/m)$, which is one for $x \in [0,m)$, and zero otherwise, can be written as

$$\varphi^0(x/m) = \sum_{k=0}^{m-1} \varphi^0(x-k) = \sum_{k\in Z} h_m^0(k)\varphi^0(x-k), \tag{28}$$

where $h_m^0(k)$ is the filter whose z-transform is $H_m^0(z) = \sum_{k=0}^{m-1} z^{-k}$ (discrete pulse of size m). By convolving this equation with itself $(n+1)$-times and performing the appropriate normalization, one finds that

$$\varphi^n(x/m) = \sum_{k\in Z} h_m^n(k)\varphi^n(x-k), \tag{29}$$

where

$$H_m^n(z) = \frac{1}{m^n}\left(H_m^0(z)\right)^{n+1} = \frac{1}{m^n}\left(\sum_{m=0}^{m-1} z^{-k}\right)^{n+1}. \tag{30}$$

This is a two-scale equation, which indicates that a B-spline of degree n dilated by m can be expressed as a linear combination of B-splines. With the appropriate phase shift, this result also carries over for centered B-splines of degree n odd; an alternative proof is given in [101]. There are two remarkable facts connected to the above result. First, the two-scale equation (29) holds for any integer m —not just powers of two, as encountered in the multiresolution theory of the wavelet transform [48], [81], [109]. Second, the refinement filter is simply the $(n+1)$-fold convolution of the discrete rectangular impulse of width m; this can be the basis for some very fast algorithms [101]. In the standard case where $m=2$, $H_2^n(z)$ is the celebrated *binomial* filter that plays a crucial role in the theory of the wavelet transform [81]. The filter coefficients appear in the Pascal triangle represented on the first page of this article. The two-scale relation is illustrated in Fig. 9 for the case of the centered B-spline of degree 1; this corresponds to the third line of Pascal's triangle.

Spline Pyramids

For constructing multiscale representations of signals, or pyramids, one usually considers scaling factors that are powers of two. The implication of the two-scale relation for $m=2$ is that the spline subspaces S_m^n, with $m=2^i$, are nested: $S_1^n \supset S_2^n \supset \cdots \supset S_{2^i}^n \cdots$.

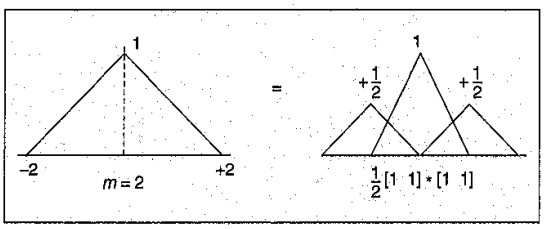

▲ 9. Illustration of the two-scale relation for the linear B-spline.

Let $P_{2^i} s = s_i$ denote the minimum error approximation of some continuously defined signal $s(x) \in L_2$ at the scale $m=2^i$. We choose to represent it by the following expansion

$$P_{2^i} s = \sum_{k\in Z} c_{2^i}(k)\varphi(x/2^i - k), \tag{31}$$

[or the $\varphi(x/2^i - k)$s are the spline basis functions at the scale $m=2^i$ (B-spline or others); they are enlarged by a factor of 2^i and spaced accordingly]. The expansion coefficients $c_{2^i}(k)$ are defined, at least formally, through the inner product (21). The interesting implication of the spline nestedness property is that the coefficients $c_{2^i}(k)$ can be computed iteratively in a very simple fashion using a combination of discrete prefiltering and down-sampling operations. The key observation is that we can obtain $P_{2^i} s = s_i$ if we simply reapproximate s_{i-1} at the next finer scale (i.e., $P_{2^i} s = P_{2^i} s_{i-1}$). Thus, we may compute the expansion coefficient as [cf. (21)]

$$c_{2^i}(k) = \frac{1}{2^i}\left\langle \sum_{l\in Z} c_{2^{i-1}}\varphi(x/2^{i-1} - l), \mathring{\varphi}(x/2^i - k)\right\rangle. \tag{32}$$

Using the two-scale relation to precompute the sequence of inner products,

$$\mathring{h}(k) := \frac{1}{2^i}\left\langle \varphi(x/2^{i-1} + k), \mathring{\varphi}(x/2^i)\right\rangle = \left\langle \varphi(x+k), \mathring{\varphi}(x/2)\right\rangle \tag{33}$$

it is not difficult to show that the $c_{2^i}(k)$ are evaluated by simple prefiltering with $\mathring{h}$ and down-sampling by a factor of two:

$$c_{2^i}(k) = (\mathring{h} * c_{2^{i-1}})(2k). \tag{34}$$

There is also a complementary "interpolation" filter h that allows the extrapolation of a coarser resolution to the next finer one. An example of such a pyramid is shown in Fig. 10, where we have used a cardinal representation; in other words, we are displaying the samples of the underlying spline images. The corresponding 2D spline model is separable, and the procedure is implemented by successive 1D filtering and decimation of the rows and columns of the image. The error arrays on the right are obtained by subtracting the next coarser approximation from the current spline approximation; it displays the loss of information introduced by image reduction. Specific filter formulas can be found in [99]; the filter coefficients and 1D approximation routines in the *C* language can also be obtained from the author on request.

Instead of minimizing the continuous L_2-error, it is also possible to construct spline pyramids that are optimal in the discrete l_2-norm [8]; practically, this amounts to a small modification of the reduction filter $\mathring{h}$ [96]. This kind of algorithm provides an efficient filter-based implementation of the technique known as *spline regression* in statistics

[2, 31, 113]. Most of the spline pyramids use symmetric filters that are centered on the origin (in fact, these are based on the centered B-splines rather that the causal ones that have been used here to simplify the argument). Recently, there has been some incentive for designing *centered* pyramids where the coarser nodes are positioned in the center of the finer ones [17]. These last structures are especially useful when dealing with image labels. It has also been shown that shifting the spline knots between levels can improve energy compaction [55].

Spline Wavelets

The L_2-spline pyramid that has been described above has all the required properties for a multiresolution analysis of L_2 in the sense defined by Mallat [50], [51]. In particular, the error bound (24) guarantees that we can approximate any L_2-function as closely as we wish by letting the scale go to zero. In the wavelet terminology, the multiresolution analysis is dense in L_2 [51]. Hence, there is no major difficulty in constructing the associated wavelet bases of L_2. Those wavelets provide a more efficient, non-redundant way of representing the difference images in Fig. 10. Since image reduction is achieved by repeated projection, the difference between two successive signal approximations $P_{2^{i-1}} f$ and $P_{2^i} f$ belong to the subspace $W_{2^i}^n$ that is the complement of $S_{2^i}^n$ with respect to $S_{2^{i-1}}^n$; i.e., $S_{2^{i-1}}^n = S_{2^i}^n \oplus W_{2^i}^n$ with $S_{2^i}^n \cap W_{2^i}^n = \{0\}$. This is where the famous wavelet $\psi(x)$ enters the scene: it generates the basis functions of the residual spaces [51], [91]

$$W_{2^i}^n = \text{span}\{\psi(x/2^i - k)\}_{k \in Z}.$$

There are many applications (e.g., coding) where it is more concise to express the residues $P_{2^{i-1}} f - P_{2^i} f \in W_{2^i}^n$ using wavelets rather than the basis functions of $V_{2^{i-1}}^n$ as has been is done in Fig. 10. An example of wavelet transform is shown in Fig. 11; this decomposition works well for image coding because it produces many very small coefficients in slowly varying image regions.

In wavelet theory, splines constitute a case apart because they give rise to the only wavelets that have a closed-form formula (piecewise polynomial). All other wavelet bases are defined indirectly by an infinite recursion (or by an infinite product in the Fourier domain) [23], [48], [81], [109]. It is, therefore, no coincidence that most of the earlier wavelet constructions were based on splines; for instance, the Haar wavelet transform (n=0) [34], the Franklin system (n=1), Strömberg's one-sided orthogonal splines [82], and the celebrated Battle-Lemarié wavelets [11], [47]. Since then, the family has grown and there are now several other subclasses of spline wavelets available; they differ in the type of projection used and in their orthogonality properties.

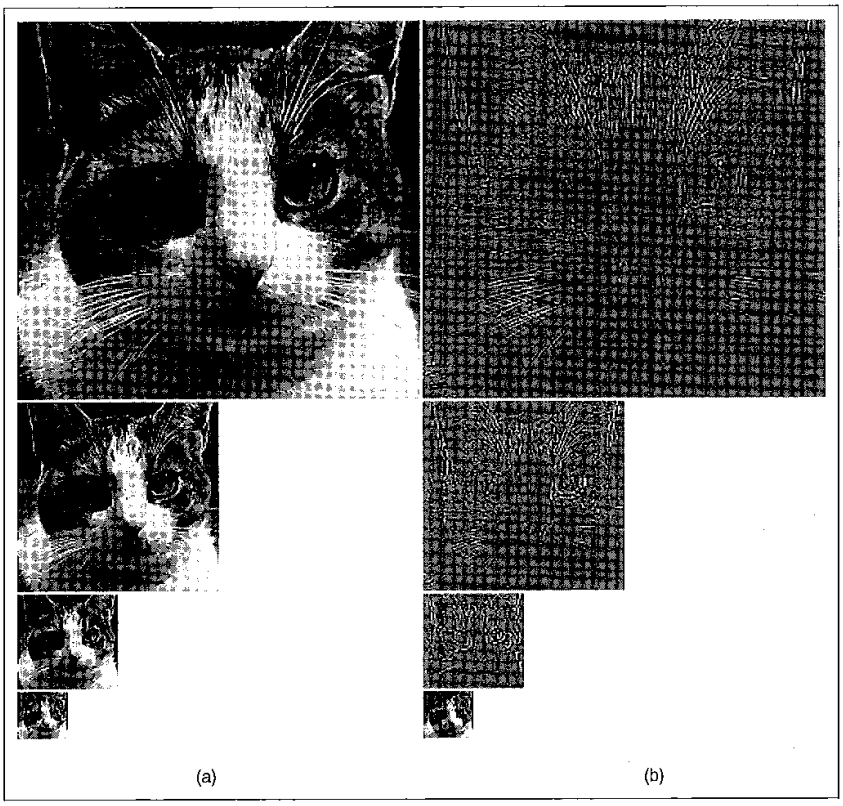

10. Cubic spline multiresolution image approximation. (a) Cubic spline pyramid $\{P_8 s, P_4 s, P_2 s, P_1 s\}$. (b) Error pyramid: $\{P_8 s - P_4 s, P_4 s - P_2 s, P_2 s - P_1 s, P_1 s\}$. What is displayed are the samples of those splines at the location of the knots (cardinal representation).

Corresponding to an orthogonal projection (and to the L_2-pyramid above) is the class of *semi-orthogonal* wavelets, which are orthogonal with respect to dilation [98]. These wavelets span the same space as the Battle-Lemarié splines, but are not constrained to be *orthogonal*. This gives flexibility and makes it possible to design wavelets with many interesting properties [5] and almost any desirable shape [1]. Of particular interest are the B-spline wavelets [20], [94], which are compactly supported and optimally localized in time and frequency; asymptotically, they achieve the lower limit specified by Heisenberg's uncertainty principle

[94]. The only downside of semi-orthogonal wavelets is that some of the corresponding wavelet filters are IIR. This is not a serious problem in practice, thanks to the availability of fast-recursive algorithms (cf. Box 2)—dealing efficiently with IIR filters is the main thrust of B-spline signal processing.

Researchers have also designed spline wavelets such that the corresponding wavelet filters are FIR [21], [108]. These *biorthogonal* wavelets are constructed using two multiresolutions instead of one, with the spline spaces on the synthesis side. The major difference with the semi-orthogonal case is that the underlying projection operators are oblique rather than orthogonal [4]. Biorthogonal spline wavelets have many desirable properties that have made them very popular for applications: they are short, symmetrical, easy to implement (FIR filterbank), and very regular. Within the biorthogonal class, there is still one possibility which is to orthogonalize the wavelets with respect to shifts, which leads to the more recent class of *shift-orthogonal* wavelets. Such a construction was first illustrated with a family of hybrid spline wavelets where the analysis and synthesis basis functions are splines of different degree n_1 and n_2 [104].

Further Optimality Properties

Variational Properties

Splines have some very interesting extremal properties. One important result is the *first integral relation* [3], which states that for any function $f(x)$ whose mth derivative is square integrable, we have

$$\int_{-\infty}^{+\infty} (f^{(m)})^2\,dx = \int_{-\infty}^{+\infty} (s^{(m)})^2\,dx + \int_{-\infty}^{+\infty} (f^{(m)} - s^{(m)})^2\,dx, \tag{35}$$

where $s(x)$ is the spline interpolant of degree $n=2m-1$ such that $s(k)=f(k)$. In particular, if we apply this decomposition to the problem of the interpolation of a given data sequence $f(k)$, we may conclude that, among all possible interpolants $f(x)$, the spline interpolant $s(x)$ is the only one that minimizes the norm of the mth derivative, which is a rather remarkable result [72]. The reason is simply that the second term in (35) is non-zero if $f(x) \neq s(x)$ at the non-integer points. In this sense, the spline is the interpolating function that oscillates the least. For $m=2$, the energy function in (35) is a good approximation to the integral of the curvature for the curve $y=f(x)$. Thus, cubic splines interpolant exhibit a *minimum curvature property*, which justifies the analogy with the draftman's spline, or French curve. The latter device is a thin elastic beam that is constrained to pass through a given set of points.

Smoothing Splines

Interpolation is not the only approach for fitting a continuous model to a signal. For noisy data, an exact fit may not even be desirable. Such situations can be dealt with by relaxing the interpolation constraint and by making best use of our a priori knowledge about the problem. The natural extension of the previous interpolation problem is to find the function $s(x)$ that minimizes

$$\sum_{k\in Z} (f(k)-s(k))^2 + \lambda \int_{-\infty}^{+\infty} (s^{(m)}(x))^2\,dx. \tag{36}$$

This is a well-posed, regularized least-squares problem where the first term quantifies the error between the model $s(x)$ and the measured data points $f(k)$; the second term imposes a smoothness constraint on the solution. The choice of a particular value of the regularization factor λ reflects our a priori information; it can be based either on the knowledge of the variance of the noise or the degree of smoothness of the signal as measured by (35). Here again, it can be shown that the optimal solution among all possible functions is a spline of degree $n=2m-1$ [65], [71]. Part of the argument follows from the first integral equation: any non-spline fit can be improved by using its spline interpolant that further reduces the second term in the criterion while keeping the same values $s(k)$ at the grid points. The solution to the above problem is called a *smoothing spline*, because it is equivalent to a special form of smoothing of the data. Similar to the exact interpolation that corresponds to the case $\lambda \to 0$, the B-spline coefficients of the smoothing spline can be computed efficiently by recursive filtering [96].

Introducing a regularization term, as in (36), is a standard practice for dealing with many other types of ill-posed problems [61], including sparse and non-equally spaced data. The regularization parameter λ is typically used to control the smoothness of the solution. For $m=1$, the regularization will tend to privilege small values of the derivative; a good physical analogy is that of a membrane that takes a constant value at equilib-

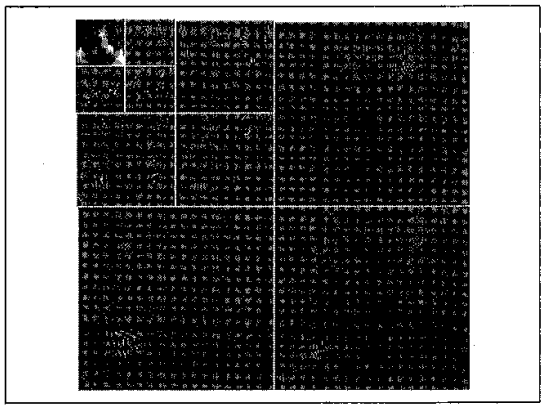

11. Separable cubic spline wavelet transform corresponding to the multiresolution decomposition in Fig. 10. The wavelet transform is implemented iteratively using a separable algorithm. First, the rows of the image are split into two halfs using a two-channel filterbank. Second, the same procedure is applied to the columns. This process is then iterated on the intermediate lower resolution images, which are precisely the ones displayed in Fig. 10a.

rium. For $m=2$, there is no penalty for linear gradients. The generalization of this problem to higher dimensions leads to another area of study called "thin-plates splines" [113]. Generalized splines and radial basis functions can also be defined in a similar way by introducing more complex regularization terms [63].

Smoothing splines are closely related to wavelet denoising techniques, which may be expressed in a regularization framework as well [19]. The main difference is that the smoothing spline is a linear estimator, while Donoho's wavelet shrinkage is non-linear [30]. The idea is simple and was pioneered by Weaver et al. using orthogonal spline wavelets [114]: take the wavelet transform of a signal and set to zero the coefficients below some critical threshold while slightly attenuating the other ones (soft-threshold); then reconstruct the signal by inverse wavelet transform. The wavelet technique has the advantage of preserving edges; it is well suited for signal or images that are piecewise smooth, and is optimal in a well-defined statistical sense [30], [48].

Best-Approximation Properties Among Wavelets

In "Controlling the Approximation Error," we saw that splines have an $L=n+1$ order of approximation, which means that the error decays like the Lth power of the sampling step. There are also non-spline functions $\varphi(x)$ that have the same property; in particular, the Lth order scaling functions encountered in the multiresolution theory of the wavelet transform. Note that, in the wavelet world, the order is usually specified by the number of vanishing moments of the analysis wavelet $\psi(x)$. An equivalent statement of the order property is that the translates of the function φ must reproduce the polynomials of degree n [26], [79]. In general, the order property implies that we have the following asymptotic form of the approximation error (cf. [89])

$$\left\|s-P_{\varphi,T}s\right\|=C_{\varphi,L}^{-}\cdot T^{L}\left\|s^{(L)}\right\|,\ \text{as } T\to 0, \tag{37}$$

where $P_{\varphi,T}s$ is the projection of s onto the space $V_T=\text{span}\{\varphi(x/T-k)\}_{k\in Z}$ and where the constant $C_{\varphi,L}^{-}$ can be determined explicitly [14], [89]. This is essentially the same equation as (24) with an equality instead of an upper bound; the asymptotic leading constant $C_{\varphi,L}^{-}$ is, therefore, necessarily smaller than C_L in (24).

Among all known wavelet families, splines appear to have the best approximation property in the sense that the magnitude of the constant $C_{\varphi,L}^{-}$ is minimum [83], [89]. This means that, in the asymptotic regime where the error is small, we can apply a coarser sampling step if we use splines as opposed to other basis functions (or wavelets) with the same order L. The potential reduction in sampling density can be quite significant. For instance, Sweldens observed that splines at half the resolution could provide a better approximation than Daubechies' wavelets [83]. Recently, the exact subsampling factor such that the asymptotic errors in both cases are identical has been determined analytically [14]; it converges to π as the order L gets sufficiently large!

Maximum Regularity and Shortest Support

It is well known from wavelet theory that the B-splines are the shortest scaling functions of order L [23], [81]. They are also the most regular ones if one takes the size of the refinement filter into account [90]: their Sobolev regularity (r derivatives in L_2) is $r_{\max}=n+\frac{1}{2}$ [81] and their Hölder exponent is $\alpha=n$ [66]. This latter property means that the B-spline of degree n is "almost" n times continuously-differentiable; strictly speaking, the nth derivative of spline of degree n has some isolated points of discontinuities (knots), but is bounded nevertheless.

If one extends the mathematical analysis to functions that do not necessarily satisfy the two-scale relation (multiresolution property), then the B-splines can still be shown to be the shortest functions of order L. However, there are also other solutions, albeit less regular [12]. Thus, in the most general sense, the B-splines are the shortest and smoothest functions of order L. Since the performance of an approximation algorithm is strongly determined by the order of approximation and to some extent by the regularity of the basis functions, this has important practical consequences, especially for image interpolation (cf. Box 3). In this type of processing, where computational cost is essentially determined by the size of the basis function, it makes perfect sense to use the shortest functions with the required order properties; i.e., the B-splines.

Fractional Splines

Interestingly, B-splines can be generalized to fractional orders (cf. the illustration on the cover of this issue) [102]. The fractional splines are piecewise power functions with building blocks of the form $(x-x_k)_+^{\alpha}$, with $\alpha>-\frac{1}{2}$ real. The corresponding B-splines provide a smooth transition between the polynomial ones. They retain all the properties of the conventional B-splines—one merely replaces n by α in all formulas, except the compact support [the finite sum in (10) becomes an infinite one]. One justification for looking at the fractional B-splines is that they offer the same conceptual ease for dealing with fractional derivatives as the conventional splines do for derivatives. One potential application is the analysis of fractional Brownian motion processes.

Applications

Our intent here is not to be exhaustive, but instead to give a brief overview of the type of signal and image processing applications that can benefit from the use of polynomial splines.

Zooming and Visualization

Image zooming and interpolation are perhaps the most obvious applications of splines. These manipulations are especially useful for medical imaging [57], [60], but also for multimedia and digital photography, which are rapidly expanding applications areas. The use of cubic splines in image processing was pioneered by Hou and Andrews [36]. The proposed approach was not yet very practical because the B-spline coefficients were determined by matrix inversion. The method was made much more efficient with the introduction of recursive filtering algorithms [93]. Note that zooming by powers of two can also be implemented using the EXPAND function of a pyramid [96].

Geometric Image Transformations

When there is no size reduction, geometric transformations are often implemented by standard spline interpolation (cf. Box 3). One of the drawbacks is that the complexity of the method, which is two-dimensional, grows rapidly with the order $L=n+1$ of the model [typically, $O(L^3)$ per pixel]. Fortunately, for the simplest transformations (scaling and rotations), there are ways to make the problem separable through a clever factorization of the transformation matrix [58]. This technique was used in [105] to design a high-quality spline-based procedure allowing the rotation of images using 1D convolutions only; it was extended in [86] to allow for affine transformations in 2D and 3D as well. For image reductions, it is preferable to use a least-squares approximation to reduce aliasing artifacts. Such an algorithm exists for re-sizing images with arbitrary scaling factors [100]—not just the usual powers of two. Recently, it has been simplified and accelerated using oblique projections [46]. The idea is to use the box function as the simplest possible prefilter, and to apply the appropriate digital filtering compensation afterward so that the resulting approximation is a projection. The results are almost indistinguishable from the least-squares solution, and the algorithm generalizes for any degree n.

Filter Design and Fast Continuous Wavelet Transform

Thanks to the m-scale relation, a signal can be convolved very efficiently with a discrete B-spline of size m using a cascade of moving average filters (recursive update). This yields an algorithm that has a complexity independent of the size of the basis functions. Thus, we have a very efficient way of implementing a scalable filter whose impulse response is the sum of a few B-spline basis functions. This is an idea that has been exploited for filter design [59], and for implementing the continuous wavelet transform with integer scales [101]. This type of algorithm achieves the lowest $O(1)$ complexity per computed coefficient. In contrast with other wavelet transform algorithms [67], the B-spline approach is non-iterative across scale and, therefore, well suited to a parallel implementation. Splines are also used to compute wavelet transforms with arbitrary non-integer scales [110]. This is more complicated because it necessitates approximating enlarged wavelets using either orthogonal [111] or oblique projections [112]. This latter option appears to be more advantageous because it simplifies the determination of the filter coefficients without any measurable degradation.

Image Compression

Image compression is another area where splines can be helpful. Most of today state-of-the-art methods use wavelets—the most prominent ones are Shapiro's embedded zero-tree wavelet coder [77], and Said and Pearlman's SPIHT [69]. While there are many possible choices of wavelet filters, many researchers tend to favor the biorthogonal splines for the reasons mentioned before (symmetry, short support, and excellent approximation properties) [9], [81]. We should also mention some non-wavelet-based systems: for example, the method of Toraichi et al., which uses quadratic spline interpolation [87], and Moulin's decomposition in terms of hierarchical spline basis functions [53]. Pyramid coders, which extend Burt and Adelson's initial idea, should not be dismissed either [39], [56], [88], [107]. These can offer advantages, especially in higher dimensions where the overhead with respect to wavelets becomes negligible. Finally, splines provide a good solution for sub-pixel motion compensation. Moulin et al. have proposed a nicely integrated system where the motion vectors are represented using hierarchical basis functions (linear splines) [54].

Multi-Scale Processing and Image Registration

Spline pyramids provide a very convenient tool for performing multiscale image processing, especially when the underlying problem is formulated in the continuous domain. This is a powerful idea for the implementation of iterative algorithms using a coarse-to-fine iteration strategy [68]. The benefits are twofold: first, there is an obvious acceleration because the cost of all low-resolution iterations is essentially negligible. Second, a multi-scale approach tends to be quite robust, which means that the algorithm is much less likely to get trapped in a local optimum. A good illustration of these ideas is provided by the image registration algorithm described in [85]. This method makes use of the same high-quality spline model for all aspects of the computation: image pyramid, geometric transform, and computation of the gradient of the criterion that is optimized. The benefits of this consistent design can be found in the results, which are the best reported so far (error less than 1/100th of a pixel in a series of controlled experiments). The approach is reasonably fast because it makes the best use of its iterations: good starting conditions with an optimizer (Marquardt-Levenberg) that is extremely efficient near the optimum.

Contour Detection

The spline formalism lends itself very naturally to the computation of gradients required for contour detection. One can, for instance, reinterpret some of the classical edge detectors from this perspective [96]. To improve the gradient estimation in the presence of noise, Poggio et al. proposed using a smoothing spline technique [61], [62]. They showed the approach to be more or less equivalent to smoothing the image with a Gaussian filter in a preprocessing step (Canny's edge detector [18]). This analogy holds even further [96]: there is an exact equivalence between a smoothing spline edge detector and Deriche's recursive formulation of Canny's edge detector [28]. Finally, Mallat and Zhong used wavelets that are derivatives of B-splines for obtaining their multi-scale edge representation of images [49].

Snakes and Contour Modeling

In computer graphics, curves are often generated using B-splines [10]. This parametric representation is also well suited to the analysis of shapes and contours [32]. In particular, it is well adapted to extracting shape invariants [22], [37]. The simplest contour splines are piecewise linear; they can be used to encode boundaries optimally in the rate-distortion sense [44], [75].

Menet et al. proposed using B-splines snakes for extracting contours in images [52]. A snake is an energy minimization spline segment with external and internal forces [43]. It simulates an elastic material that can dynamically conform to local image features. The internal forces act as a regularization device by constraining the rigidity of the curve. Alternatively, the smoothness of the curve can also be controlled directly and more simply by adapting the scale of the basis functions [16].

Analog-to-Digital Conversion

Spline and wavelet sampling present interesting alternatives to the conventional approach dictated by Shannon's sampling theorem. These techniques can be adapted for dealing with non-ideal acquisition devices [92], and multi-channel measurements [106]. With this more general view of sampling, it is tempting to modify the acquisition scheme so as to measure the coefficients of some signal expansion (i.e., to perform some prescribed inner products) rather than to measure the samples of the signal itself. Healy and Weaver have pioneered this idea for magnetic resonance imaging [35], [114]. They proposed a wavelet-encoding scheme using separable basis functions (Battle-Lemarié splines along the x-dimension, and conventional Fourier exponentials along the y-direction). Splines are also useful for the converse task of digital-to-analog conversion. Kamada et al. designed a quadratic spline signal generator [41], [42]; one of their circuits was used commercially for high-fidelity sound reproduction.

Conclusion

We hope to have convinced the reader that splines constitute a useful tool for signal processing. Their main advantages can be summarized as follows:

▲ One can always obtain a continuous representation of a discrete signal by fitting it with a spline in one or more dimensions. The fit may be exact (interpolation) or approximate (least-squares or smoothing splines). Spline fits are usually preferable to other forms of representations (e.g., Lagrange polynomial interpolation) because they have less of a tendency to oscillate (minimum curvature property).

▲ Polynomial splines can be expressed as linear combinations of B-spline basis functions. For equally spaced knots, the spline parameters (B-spline coefficients) may be determined by simple digital filtering. There is no need for matrix manipulations!

▲ The primary reason for working with the B-spline representation is that the B-splines are compactly supported. They are the shortest functions with an order of approximation $L=n+1$. This short support property is a key consideration for computational efficiency. Their simple analytical form also greatly facilitates manipulations.

▲ Splines are smooth and well-behaved functions (piecewise polynomials). Splines of degree n are $(n\text{-}1)$ continuously differentiable. As a result, splines have excellent approximation properties. Precise convergence rates and error estimates are available.

▲ Splines have multiresolution properties that make them very suitable for constructing wavelet bases and for performing multi-scale processing.

▲ B-splines and their wavelet counterparts have excellent localization properties; they are good templates for time-frequency signal analysis.

▲ The family of polynomial splines provides design flexibility. By increasing the degree n, we progressively switch from the simplest piecewise constant $(n=0)$ and piecewise linear $(n=1)$ representations to the other extreme, which corresponds to a band-limited signal model $(n \rightarrow +\infty)$.

▲ The conventional sampling procedure can be easily modified to obtain a spline representation of an analog signal. This essentially amounts to replacing Shannon's ideal low-pass filter with another optimal prefilter specified by the representation. In principle, there is no compelling reason other than history for preferring the band-limited model—and its corresponding sinc interpolator—over other ones.

Finally, similar spline techniques are also available for non-uniformly spaced data. The price to pay, however, is that one loses the convenient shift-invariant structure (filters) that was emphasized in this article. The reader who wishes to learn more about non-uniform splines is referred to [24] and [74].

Acknowledgments

The author would like to thank his collaborators and friends, Akram Aldroubi, Thierry Blu, Murray Eden, and Philippe Thévenaz for their invaluable help in researching splines. He is grateful to Manuela Feilner, Stefan Horbelt, Jan Kybic, Arun Kumar, Arrate Muñoz, and Daniel Sage for their constructive comments on the manuscript.

The author is much indebted to Annette Unser for her artistic interpretation of the fractional B-splines (cover) and her colorful illustration of the two-scale relation (Pascal's triangle).

Michael Unser is a professor of image processing at the Swiss Federal Institute of Technology (EPFL) in Lausanne, Switzerland. His main research area is biomedical imaging. He has a strong interest in sampling theories, multiresolution algorithms, wavelets, and the use of splines for image processing. In January 1999, he was elected Fellow of the IEEE with the citation: "for contributions to the theory and practice of splines in signal processing."

More information, including spline demos and art, can be found at http://bigwww.epfl.ch/.

References

[1] P. Abry and A. Aldroubi, "Designing multiresolution analysis-type wavelets and their fast algorithms," *J. Fourier Analysis and Applications*, vol. 2, no. 2, pp. 135-159, 1995.

[2] G.G. Agarwal, "Splines in statistics," *Bull. Allahabad Math.Soc.*, vol. 4, pp. 1-55, 1989.

[3] J.H. Ahlberg, E.N. Nilson, and J.L. Walsh, *The Theory of Splines and Their Applications*, New York: Academic Press, 1967.

[4] A. Aldroubi, "Oblique projections in atomic spaces," *Proc. Amer. Math. Soc.*, vol. 124, no. 7, pp. 2051-2060, 1996.

[5] A. Aldroubi and M. Unser, "Families of multiresolution and wavelet spaces with optimal properties," *Numerical Functional Analysis and Optimization*, vol. 14, no. 5-6, pp. 417-446, 1993.

[6] A. Aldroubi and M. Unser, "Sampling procedures in function spaces and asymptotic equivalence with Shannon's sampling theory," *Numer. Funct. Anal. and Optimiz.*, vol. 15, no. 1 & 2, pp. 1-21, 1994.

[7] A. Aldroubi, M. Unser, and M. Eden, "Cardinal spline filters: stability and convergence to the ideal sinc interpolator," *Signal Processing*, vol. 28, no. 2, pp. 127-138, 1992.

[8] A. Aldroubi, M. Unser, and M. Eden, "Discrete spline filters for multiresolutions and wavelets of l_2," *SIAM J. Math. Anal.*, vol. 25, no. 5, pp. 1412-1432, 1994.

[9] M. Antonini, M. Barlaud, P. Mathieu, and I. Daubechies, "Image coding using wavelet transform," *IEEE Trans. Image Processing*, vol. 1, no. 2, pp. 205-220, 1992.

[10] R.H. Bartels, J.C. Beatty, and B.A. Barsky, *Splines for Use in Computer Graphics*, Los Altos, CA: Morgan Kaufmann, 1987.

[11] G. Battle, "A block spin construction of ondelettes, Part I: Lemarié functions," *Commun. Math. Phys.*, vol. 110, pp. 601-615, 1987.

[12] T. Blu and M. Unser, "Minimum support interpolators with optimum approximation properties," in *Proc. Int. Conf. Image Processing*, Santa Barbara, CA, 1998, vol. III, pp. 242-245.

[13] T. Blu and M. Unser, "Approximation error for quasi-interpolators and (multi-) wavelet expansions," *Applied and Computational Harmonic Analysis*, vol. 6, no. 2, pp. 219-251, 1999.

[14] T. Blu and M. Unser, "Quantitative Fourier analysis of approximation techniques: Part II-wavelets," *IEEE Trans. Signal Processing*, vol. 47, no. 10, pp. 2796-2806.

[15] T. Blu and M. Unser, "Quantitative Fourier analysis of approximation techniques: Part I-interpolators and projectors," *IEEE Trans. Signal Processing*, vol. 47, no. 10, pp. 2783-2795.

[16] P. Brigger, J. Hoeg, and M. Unser, "B-spline snakes: a flexible tool for parametric contour detection," *IEEE Trans. Image Processing*, in press.

[17] P. Brigger, F. Müller, K. Illgner, and M. Unser, "Centered pyramids," *IEEE Trans. Image Processing*, vol. 6, no. 9, pp. 1254-1264.

[18] J.F. Canny, "A computational approach to edge detection," *IEEE Trans. Pattern Anal. Machine Intell.*, vol. PAMI-8, no. 6, pp. 679-697, 1986.

[19] A. Chambolle, R.A. DeVore, N.-Y. Lee, and B.J. Lucier, "Nonlinear wavelet image processing: variational problems, compression, and noise removal through wavelet shrinkage," *IEEE Trans. Image Processing*, vol. 7, no. 33, pp. 319-335, 1998.

[20] C.K. Chui and J.Z. Wang, "On compactly supported spline wavelets and a duality principle," *Trans. Amer. Math. Soc.*, vol. 330, no. 2, pp. 903-915, 1992.

[21] A. Cohen, I. Daubechies, and J.C. Feauveau, "Bi-orthogonal bases of compactly supported wavelets," *Comm. Pure Appl. Math.*, vol. 45, pp. 485-560, 1992.

[22] F.S. Cohen, Z. Huang, and Z. Yang, "Invariant matching and identification of curves using B-splines curve representation," *IEEE Trans. Image Processing*, vol. 4, no. 1, pp. 1-10, 1995.

[23] I. Daubechies, *Ten Lectures on Wavelets*, Philadelphia, PA: Society for Industrial and Applied Mathematics, 1992.

[24] C. de Boor, "On calculating with B-splines," *J. Approximation Theory*, vol. 6, pp. 50-62, 1972.

[25] C. de Boor, *A Practical Guide to Splines*, New York: Springer-Verlag, 1978.

[26] C. de Boor, "The polynomials in the linear span of integer translates of a compactly supported function," *Constructive Approximation*, vol. 3, pp. 199-208, 1987.

[27] C. de Boor, K. Höllig, and S. Riemenschneider, "Bivariate cardinal interpolation by splines on a three-direction mesh," *IL J. Mathematics*, vol. 29, no. 4, pp. 533-566, 1985.

[28] R. Deriche, "Using Canny's criteria to derive a recursively implemented optimal edge detector," *Int. J. Comput. Vis.*, vol. 1, no. 2, pp. 167-187, 1987.

[29] P. Dierckx, *Curve and Surface Fitting With Splines*, Oxford: Oxford University Press, 1995.

[30] D.L. Donoho, "De-noising by soft-thresholding," *IEEE Trans. Information Theory*, vol. 41, no. 3, pp. 613-627, 1995.

[31] R.L. Eubank, "Approximate regression models and splines," *Commun. Stat. Theory Math.*, vol. 13, pp. 433-484, 1984.

[32] M. Flickner, J. Halner, E.J. Rodríguez, and J.L.C. Sanz, "Periodic quasi-orthogonal spline bases and applications to least-squares curve fitting of digital images," *IEEE Trans. Image Processing*, vol. 5, no. 1, pp. 71-88, 1996.

[33] A. Goshtasby, F. Cheng, and B.A. Barsky, "B-spline curves and surfaces viewed as digital filters," *Computer Vision, Graphics, and Image Processing*, vol. 52, pp. 264-275, 1990.

[34] A. Haar, "Zur Theorie der orthogonalen Funktionensysteme," *Math. Ann.*, vol. 69, pp. 331-371, 1910.

[35] D.M. Healy, Jr. and J.B. Weaver, "Two applications of wavelet transforms in magnetic resonance," *IEEE Trans. Information Theory*, vol. 38, no. 2, pp. 840-860, 1992.

[36] H.S. Hou and H.C. Andrews, "Cubic splines for image interpolation and digital filtering," *IEEE Trans. Acoust., Speech, and Signal Processing*, vol. ASSP-26, no. 6, pp. 508-517, 1978.

[37] Z. Huang and F.S. Cohen, "Affine-invariant B-spline moments for curve matching," *IEEE Trans. Image Processing*, vol. 5, no. 10, pp. 1473-1480, 1996.

[38] R. Hummel, "Sampling for spline reconstruction," *SIAM J. Appl. Math.*, vol. 43, no. 2, pp. 278-288, 1983.

[39] K. Illgner and F. Müller, "Scalable video coding at very low bit rates employing resolution pyramids," in *Proc. EUSIPCO-96*, Trieste, Italy, 1996, vol. 2, pp. 1343-1346.

[40] R.-Q. Jia and J. Lei, "Approximation by multi-integer translates of functions having global support," *J. Approximation Theory*, vol. 72, no. 2-23, 1993.

[41] M. Kamada, K. Toraichi, and R.E. Kalman, "A smooth signal generator based on quadratic B-spline functions," *IEEE Trans. Signal Processing*, vol. 43, no. 5, pp. 1252-1255, 1995.

[42] M. Kamada, K. Toraichi, and R.E. Kalman, "Quadratic spline interpolator," *Int. J. Systems Science*, vol. 27, no. 10, pp. 977-983, 1996.

[43] M. Kass, A. Witkin, and D. Terzopoulos, "Snakes: active contour models," *Int. J. Comput. Vision*, vol. 1, pp. 321-331, 1987.

[44] A.K. Katsaggelos, L.P. Kondi, F.W. Meier, J. Ostermann, and G.M. Schuster, "MPEG-4 and Rate-Distortion-Based Shape-Coding Techniques," *Proc. IEEE*, vol. 86, no. 6, pp. 1126-1154, 1998.

[45] P. Lancaster and K. Salkauskas, *Curve and Surface Fitting: An Introdution*, London: Academic Press, 1986.

[46] C. Lee, M. Eden, and M. Unser, "High quality image re-sizing using oblique projection operators," *IEEE Trans. Image Processing*, vol. 7, no. 5, pp. 679-692, 1998.

[47] P.-G. Lemarié, "Ondelettes à localisation exponentielles," *J. Math. pures et appl.*, vol. 67, no. 3, pp. 227-236, 1988.

[48] S. Mallat, *A Wavelet Tour of Signal Processing*, San Diego: Academic Press, 1998.

[49] S. Mallat and S. Zhong, "Characterization of signals from multiscale edges," *IEEE Trans. Patt. Anal. Machine Intell.*, vol. 14, no. 7, pp. 710-732, 1992.

[50] S.G. Mallat, "Multiresolution approximations and wavelet orthogonal bases of $L^2(R)$," *Trans. Amer. Math. Soc.*, vol. 315, no. 1, pp. 69-87, 1989.

[51] S.G. Mallat, "A theory of multiresolution signal decomposition: the wavelet representation," *IEEE Trans. Pattern Anal. Machine Intell.*, vol. PAMI-11, no. 7, pp. 674-693, 1989.

[52] S. Menet, P. Saint-Marc, and G. Medioni, "B-snakes: implementation and application to stereo," in *Proc. Image Understanding Workshop*, DARPA, 1990, 720-726.

[53] P. Moulin, "A multiscale relaxation algorithm for SNR maximization in nonorthogonal subband coding," *IEEE Trans. Image Processing*, vol. 4, no. 9, pp. 1269 - 1281, 1995.

[54] P. Moulin, R. Krishnamurthy, and J.W. Woods, "Multiscale modeling and estimation of motion fields for video coding," *IEEE Transactions on Image Processing*, vol. 6, no. 12, pp. 1606-1620, 1997.

[55] F. Müller, P. Brigger, K. Illgner, and M. Unser, "Multiresolution approximation using shifted splines," *IEEE Trans. Signal Processing*, vol. 46, no. 9, pp. 2555-2558, 1998.

[56] F. Müller and K. Illgner, "Embedded Laplacian pyramid image coding using conditional arithmetic coding," in *Proc. Int. Conf. Image Processing*, Lausanne, Switzerland, 1996, vol. 1, pp. 221-224.

[57] J.L. Ostuni, A.K.S. Santha, V.S. Mattay, D.R. Weinberger, R.L. Levin, and J.A. Frank, "Analysis of interpolation effects in the reslicing of functional MR-images," *J. Computer Assisted Tomography*, vol. 21, no. 5, pp. 803-810, 1997.

[58] A.W. Paeth, "A fast algorithm for general raster rotation," *in Proc. Graphics Interface '86 - Vision Interface '86*, 1986, 77-81.

[59] D. Pang, L.A. Ferrari, and P.V. Sankar, "B-spline FIR filters," *Circuits, Systems, and Signal Processing*, vol. 13, no. 1, pp. 31-64, 1994.

[60] J.A. Parker, R.V. Kenyon, and D.E. Troxel, "Comparison of interpolating methods for image resampling," *IEEE Trans. Med. Imaging*, vol. MI-2, no. 1, pp. 31-39, 1983.

[61] T. Poggio, V. Torre, and C. Koch, "Computational vision and regularization theory," *Nature*, vol. 317, pp. 314-319, 1985.

[62] T. Poggio, H. Voorhees, and A. Yuille, "A regularized solution to edge detection," *Journal of Complexity*, vol. 4, no. 2, pp. 106-123, 1988.

[63] M.J.D. Powell, "The theory of radial basis function approximation in 1990," in *Advances in Numerical Analysis II: Wavelets, Subdivision Algorithms and Radial Functions*, W.A. Light, Ed., Oxford, U.K.: Oxford Univ. Press, pp. 105-210, 1992.

[64] P.M. Prenter, *Splines and Variational Methods*, New York: Wiley, 1975.

[65] C.H. Reinsh, "Smoothing by spline functions," *Numer. Math.*, vol. 10, pp. 177-183, 1967.

[66] O. Rioul, "Simple regularity criteria for subdivision schemes," *SIAM J. Math. Anal.*, vol. 23, pp. 1544-1576, 1992.

[67] O. Rioul and P. Duhamel, "Fast algorithms for discrete and continuous wavelet transforms," *IEEE Trans Information Theory*, vol. IT-38, no. 2, pp. 569-586, 1992.

[68] A. Rosenfeld, *Multiresolution Image Processing*, New York: Springer-Verlag, 1984.

[69] A. Said and W.A. Pearlman, "A new fast and efficient image codec based on set partitioning in hierarchical trees," *IEEE Trans. Circuits Syst. Video Technol.*, vol. 6, pp. 243-250, 1996.

[70]I.J. Schoenberg, "Contribution to the problem of approximation of equidistant data by analytic functions," *Quart. Appl. Math.*, vol. 4, pp. 45-99, 112-141, 1946.

[71] I.J. Schoenberg, "Spline functions and the problem of graduation," *Proc. Nat. Acad. Sci.*, vol. 52, pp. 947-950, 1964.

[72] I.J. Schoenberg, *Cardinal Spline Interpolation*, Philadelphia, PA: Society of Industrial and Applied Mathematics, 1973.

[73] I.J. Schoenberg, "Notes on spline functions III: on the convergence of the interpolating cardinal splines as their degree tends to infinity," *Israel J. Math.*, vol. 16, pp. 87-92, 1973.

[74] L.L. Schumaker, *Spline Functions: Basic Theory*, New York: Wiley, 1981.

[75] G.M. Schuster, G. Melnikov, and A.K. Katsaggelos, "Operationally optimal vertex-based shape coding," *IEEE Signal Processing Magazine*, vol. 15, no. 6, pp. 91-108, 1998.

[76] C.E. Shannon, "Communication in the presence of noise," *Proc. I.R.E.*, vol. 37, pp. 10-21, 1949.

[77] J. Shapiro, "Embedded image coding using zerotrees of wavelet coefficients," *IEEE Trans. Acoustics, Speech and Signal Processing*, vol. 41, no. 12, pp. 3445-3462, 1993.

[78] D. Slepian, "On bandwidth," *Proc. IEEE*, vol. 64, no. 3, pp. 292-300, 1976.

[79] G. Strang, "Wavelets and dilation equations: a brief introduction," *SIAM Review*, vol. 31, pp. 614-627, 1989.

[80] G. Strang and G. Fix, "A Fourier analysis of the finite element variational method," in *Constructive Aspect of Functional Analysis*, Rome: Edizioni Cremonese, pp. 796-830, 1971.

[81] G. Strang and T. Nguyen, *Wavelets and Filter Banks*, Wellesley, MA: Wellesley-Cambridge, 1996.

[82] J.O. Strömberg, "A modified Franklin system and higher-order spline system of R^n as unconditional bases for Hardy spaces," *in Proc. Conference in Harmonic Analysis* in honor of Antoni Zygmund, 1983, vol. II, pp. 475-493.

[83] W. Sweldens and R. Piessens, "Asymptotic error expansions for wavelet approximations of smooth functions II," *Numer. Math.*, vol. 68, no. 3, pp. 377-401, 1994.

[84] P. Thévenaz, T. Blu, and M. Unser, "Image interpolation and resampling," in *Handbook of Medical Image Processing*, in press.

[85] P. Thévenaz, U.E. Ruttimann, and M. Unser, "A pyramid approach to subpixel registration based on intensity," *IEEE Trans. Image Processing*, vol. 7, no. 1, pp. 27-41, 1998.

[86] P. Thévenaz and M. Unser, "Separable least-squares decomposition of affine transformations," in *Proc. IEEE Int. Conf. on Image Processing*, Santa Barbara, October 26-29, 1997, CD-ROM paper no. 200.

[87] K. Toraichi, S. Yang, M. Kamada, and R. Mori, "Two-dimensional spline interpolation for image reconstruction," *Pattern Recognition*, vol. 21, no. No. 3, pp. 275-284, 1988.

[88] M. Unser, "An improved least squares Laplacian pyramid for image compression," *Signal Processing*, vol. 27, no. 2, pp. 187-203, 1992.

[89] M. Unser, "Approximation power of biorthogonal wavelet expansions," *IEEE Trans. Signal Processing*, vol. 44, no. 3, pp. 519-527, 1996.

[90] M. Unser, "Ten good reasons for using spline wavelets," *Proc. SPIE* vol. 3169, Wavelet Applications in Signal and Image Processing V, San Diego, CA, August 6-9, 1997, pp. 422-431.

[91] M. Unser and A. Aldroubi, "Polynomial splines and wavelets-A signal processing perspective," in *Wavelets-A Tutorial in Theory and Applications*, C.K. Chui, Ed., San Diego: Academic Press, pp. 91-122, 1992.

[92] M. Unser and A. Aldroubi, "A general sampling theory for non-ideal acquisition devices," *IEEE Trans. Signal Processing*, vol. 42, no. 11, pp. 2915-2925, 1994.

[93] M. Unser, A. Aldroubi, and M. Eden, "Fast B-spline transforms for continuous image representation and interpolation," *IEEE Trans. Pattern Anal. Machine Intell.*, vol. 13, no. 3, pp. 277-285, 1991.

[94] M. Unser, A. Aldroubi, and M. Eden, "On the asymptotic convergence of B-spline wavelets to Gabor functions," *IEEE Trans. Information Theory*, vol. 38, no. 2, pp. 864-872, 1992.

[95] M. Unser, A. Aldroubi, and M. Eden, "Polynomial spline signal approximations: filter design and asymptotic equivalence with Shannon's sampling theorem," *IEEE Trans. Information Theory*, vol. 38, no. 1, pp. 95-103, 1992.

[96] M. Unser, A. Aldroubi, and M. Eden, "B-spline signal processing: Part II-efficient design and applications," *IEEE Trans. Signal Processing*, vol. 41, no. 2, pp. 834-848, 1993.

[97] M. Unser, A. Aldroubi, and M. Eden, "B-spline signal processing: Part I-theory," *IEEE Trans. Signal Processing*, vol. 41, no. 2, pp. 821-833, 1993.

[98] M. Unser, A. Aldroubi, and M. Eden, "A family of polynomial spline wavelet transforms," *Signal Processing*, vol. 30, no. 2, pp. 141-162, 1993.

[99] M. Unser, A. Aldroubi, and M. Eden, "The L_2 polynomial spline pyramid," *IEEE Trans. Pattern Anal. Mach. Intell.*, vol. 15, no. 4, pp. 364-379, 1993.

[100] M. Unser, A. Aldroubi, and M. Eden, "Enlargement or reduction of digital images with minimum loss of information," *IEEE Trans. Image Processing*, vol. 4, no. 3, pp. 247-258, 1995.

[101] M. Unser, A. Aldroubi, and S.J. Schiff, "Fast implementation of the continuous wavelet transform with integer scales," *IEEE Trans. Signal Processing*, vol. 42, no. 12, pp. 3519-3523, 1994.

[102] M. Unser and T. Blu, "Fractional splines and wavelets," *SIAM Review*, in press.

[103] M. Unser and I. Daubechies, "On the approximation power of convolution-based least squares versus interpolation," *IEEE Trans. Signal Processing*, vol. 45, no. 7, pp. 1697-1711, 1997.

[104] M. Unser, P. Thévenaz, and A. Aldroubi, "Shift-orthogonal wavelet bases using splines," *IEEE Signal Processing Letters*, vol. 3, no. 3, pp. 85-88, 1996.

[105] M. Unser, P. Thévenaz, and L. Yaroslavsky, "Convolution-based interpolation for fast, high-quality rotation of images," *IEEE Trans. Image Processing*, vol. 4, no. 10, pp. 1371-1381, 1995.

[106] M. Unser and J. Zerubia, "A generalized sampling without bandlimiting constraints," *IEEE Trans. Circuits and Systems II: Analog and Digital Signal Processing*, vol. 45, no. 8, pp. 959-969, 1998.

[107] K.M. Uz, M. Vetterli, and D.J. LeGall, "Interpolative multiresolution coding of advanced television with compatible subchannel," *IEEE Trans. Circuits Syst. Video Tech.*, vol. 1, no. 1, pp. 86-99, 1991.

[108] M. Vetterli and C. Herley, "Wavelets and filter banks: theory and design," *IEEE Trans. Signal Processing*, vol. 40, no. 9, pp. 2207-2232, 1992.

[109] M. Vetterli and J. Kovacevic, *Wavelets and Subband Coding*, Englewood Cliffs, NJ: Prentice Hall, 1995.

[110] M.J. Vrhel, C. Lee, and M. Unser, "Comparison of algorithms for the fast computation of the continuous wavelet transform," *Proc. SPIE*, vol. 2825,Wavelet Applications in Signal and Image Processing IV, Denver, CO, August 6-9, 1996, pp. 422-431.

[111] M.J. Vrhel, C. Lee, and M. Unser, "Fast continuous wavelet transform: a least squares formulation," *Signal Processing*, vol. 57, no. 2, pp. 103-119, 1997.

[112] M.J. Vrhel, C. Lee, and M. Unser, "Rapid computation of the continuous wavelet transform by oblique projection," *IEEE Trans. Signal Processing*, vol. 45, no. 4, pp. 891-900, 1997.

[113] G. Wahba, *Spline Models for Observational Data*," Philadelphia: Society for Industrial and Applied Mathematics, 1990.

[114] J.B. Weaver, X. Yansun, D.M. Healy, and J.R. Driscoll, "Filtering noise from images with wavelet transforms," *Magnetic Resonance in Medicine*, vol. 21, no. 2, pp. 288-95, 1991.